

OFR 46-84

TUSCALOOSA RESEARCH CENTER

Open File Report 46-84



DEVELOPMENT OF A PHASE DIFFERENCE OF ARRIVAL TECHNIQUE FOR LOCATION OF TRAPPED MINERS

by

W. G. Hopkins, III

R. H. Church

W. E. Webb

BUREAU OF MINES, TUSCALOOSA, ALABAMA

Research at the Tuscaloosa Research center is carried out under a memorandum of agreement between the Bureau of Mines, U.S. Department of the Interior and the University of Alabama.

**UNITED STATES
DEPARTMENT OF
THE INTERIOR**

Open File Report #46-84

Development of a Phase Difference of Arrival Technique For Location
of Trapped Miners

by W. G. Hopkins, III, R. H. Church, and W. E. Webb
Tuscaloosa Research Center, University, Ala.

UNITED STATES DEPARTMENT OF THE INTERIOR

BUREAU OF MINES

Research at the Tuscaloosa Research Center is carried out under a memorandum of agreement between the Bureau of Mines, U.S. Department of the Interior, and the University of Alabama.

4 . 2

CONTENTS

	<u>Page</u>
List of abbreviations.....	3
Abstract.....	4
Introduction.....	5
Summary of current systems.....	5
The phase difference of arrival technique (PDOAT).....	12
Sample calculations using PDOAT.....	18
Development of the PDOAT system.....	19
Recommendations.....	25
References.....	27
Appendix A. - Fortran program for estimating phase angle through overburden.....	29
Appendix B. - Fortran program for determining the location (x, y, z coordinates) of the trapped miner.....	35

ILLUSTRATIONS

1. Seismic system.....	6
2. Electromagnetic direction-finding system.....	8
3. Electromagnetic vector field measurement technique.....	10
4. PDOAT system.....	11
5. PDOAT array with nomenclature.....	13
6. Flow chart of PDOAT algorithm.....	17
7. Block diagram of preliminary PDOAT receiver.....	20
8. Schematic diagram of high-impedance balanced input amplifier.....	21
9. Schematic diagram of narrow band-pass filter using twin-tee feedback.....	22
10. Photograph of PDOAT system components.....	23
11. Photograph of USBM personnel depolying PDOAT receiver...	24
12. Block diagram of phase-lock loop receiver.....	26

TABLES

1. Estimated position resolution, m.....	16
2. Sensor coordinates.....	18

LIST OF ABBREVIATIONS

cm centimeter

ft foot

Hz hertz

k Ω kilohm

m meter

M Ω megaohm

μ F microfarad

Ω ohm

sq mi square mile.

DEVELOPMENT OF A PHASE DIFFERENCE OF ARRIVAL TECHNIQUE

FOR LOCATION OF TRAPPED MINERS

By W. G. Hopkins, III,¹ R. H. Church,² and W. E. Webb³

*** ABSTRACT

The development of systems for location of miners who have become entrapped following a mine disaster has been one of the major research goals in the Bureau of Mines. This study details the preliminary development of such a system. Current technologies for locating trapped miners from the surface are either simple direction finders or time difference pulse systems that have accuracy limitations. Developing technologies using full vector field measurements at several receiving points are currently being studied. The necessity of measuring field strength with great accuracy can be a drawback in these systems. A system that operates with continuous wave radio signals, whose phase differences can be measured accurately even in weak signal conditions, greatly improves the location accuracy. A microcomputer would be used, in conjunction with the system, to gather and manipulate the data to automatically pinpoint the location of the trapped miner. Comparison of this system with existing technology indicates a favorable accuracy/complexity ratio for the phase difference of arrival technique.

¹Electrical engineer (faculty).

²Mining engineer.

³Physical scientist.

Tuscaloosa Research Center, Bureau of Mines, Tuscaloosa, AL

INTRODUCTION

The Bureau of Mines, under its mission to advance the safety of American miners, has undertaken and sponsored research on through-the-earth location and communication systems for many years. Experience in postdisaster rescue work has indicated a need for a reliable means of quickly locating trapped miners. This was particularly evident after the 1968 disaster at the Consol No. 9 Mine in Farmington, W. Va., where for several days the whereabouts and condition of 76 men were unknown. The Farmington disaster prompted the enactment of the Coal Mine Health and Safety Act of 1969. The tragedy at Farmington focussed national attention upon the problems of mine safety, and particularly upon those of postdisaster rescue. At the request of the Bureau of Mines, the National Academy of Engineering created the Committee on Mine Rescue and Survival Techniques to "conduct a study program to assess the technological capabilities that can be applied to survival and rescue techniques following mine disasters." The Bureau of Mines was particularly interested in the possible application of new technology to the problem of mine safety. The Committee on Mine Rescue and Survival made numerous recommendations for research and development in communications and mine rescue. The suggestions in regard to communication systems led to several Bureau of Mines programs to develop through-the-earth communications and trapped miner location systems. The phase difference of arrival technique (PDOAT) offers a new means of such location. The findings presented in this report indicate that such a system is feasible.

*** SUMMARY OF CURRENT SYSTEMS

Operation of a seismic subsurface system (1)³ is illustrated in figure 1. As reported by Westinghouse Electric Corp., the trapped miner pounds the ground by banging a hammer, rock, or similar object onto the rocky mine floor. This pounding causes vibrations in the ground which are transmitted to the surface where they are sensed by receiving transducers called geophones. Multiple geophones are positioned together for noise cancellation purposes in a form called a subarray. Seven different subarrays are strategically placed at known locations over the mine, covering an area with typically a 1,000 ft radius.

The signals received by the subarrays are transmitted either through cable or radio to an instrument van which houses the electronic location equipment. Here the signals are processed and, knowing the subarray locations and the time of arrival of the signals at each subarray, the location of the trapped miner is determined by computer.

³Underlined numbers in parentheses refer to the list of references at the end of this report.

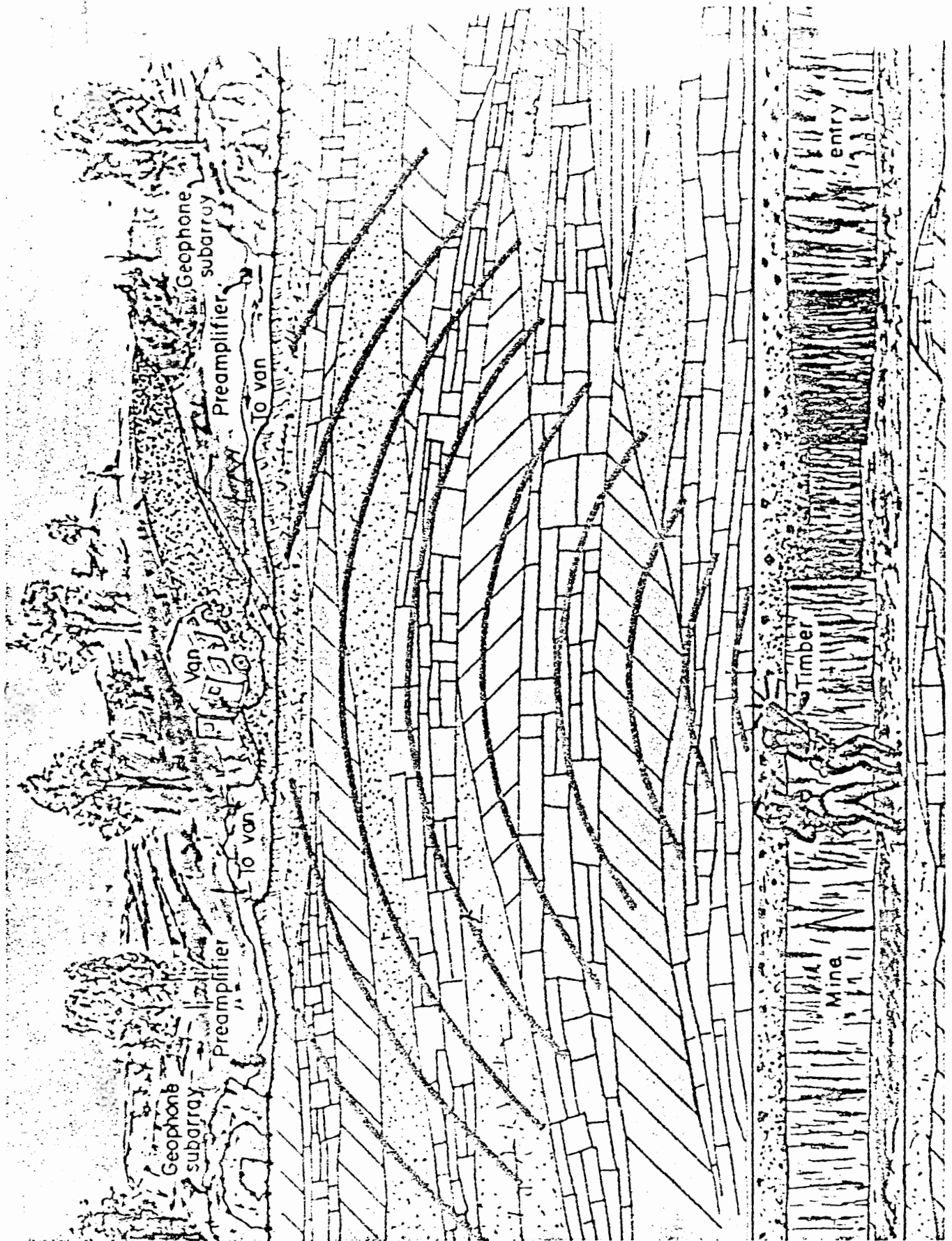


FIGURE 1
FIGURE 1

During a period of over 10 years, this system has been tested, improved, and refined. Studies were conducted at a number of coal mines throughout the United States to determine the ability of the system to detect typical signals from a miner pounding underground and thereby locate the miner's position.

The results of these tests have determined that, over a hypothetical area of confinement of 1 sq mi, there is a 0.85 probability of detecting the signal from a miner at a depth of 2,000 ft anywhere within this area (6).

The components of an electromagnetic direction-finding (EMDF) system for subsurface location are shown in figure 2. Position finding is based upon the principle that even in the presence of horizontally layered changes in ground conductivity, a buried vertical magnetic dipole produces a vertical magnetic-field vector on the surface point directly above the dipole (5).

Systems for coal-mine applications use signals in the 600 to 3,000 Hz range to maximize the signal-to-noise ratio at the surface. The trapped miner carries a small transmitter-and-antenna package. In the event of a disaster, the mine worker must deploy the antenna, preferably by wrapping it around a coal pillar to produce a 30 m by 30 m one-turn loop. The terminals of the loop antenna are then connected to the transmitter, which is powered by the miner's cap lamp battery. One variation includes a receiver in the miner's unit; and the ability to answer simple yes or no questions by keying the transmitter is also part of the design.

Location of the subsurface transmitter requires finding the location of the vertical magnetic-field component. A helicopter with an ultra low frequency (ULF) receiver first searches the mining area to determine an approximate location. A man-portable receiver is then used to determine the exact location of the null.

The electromagnetic direction-finding system provides a previously unavailable measure of safety to the miner. However, several factors should be considered, including:

(1) The accuracy with which the null in the horizontal magnetic field locates the underground beacon is dependent upon the horizontal uniformity of the rock structure. Deviations from horizontal layering (for example, surface slope) may cause errors in the location estimate. While corrections for such things as surface tilt can be made for a homogeneous earth, their use with complicated or unknown earth structures becomes difficult and may be impractical.

(2) The accuracy with which the null locates the underground beacon is also dependent upon the underground antenna being perfectly level. A nonlevel mine floor produces a tilted magnetic dipole and therefore may introduce errors in the position estimate.

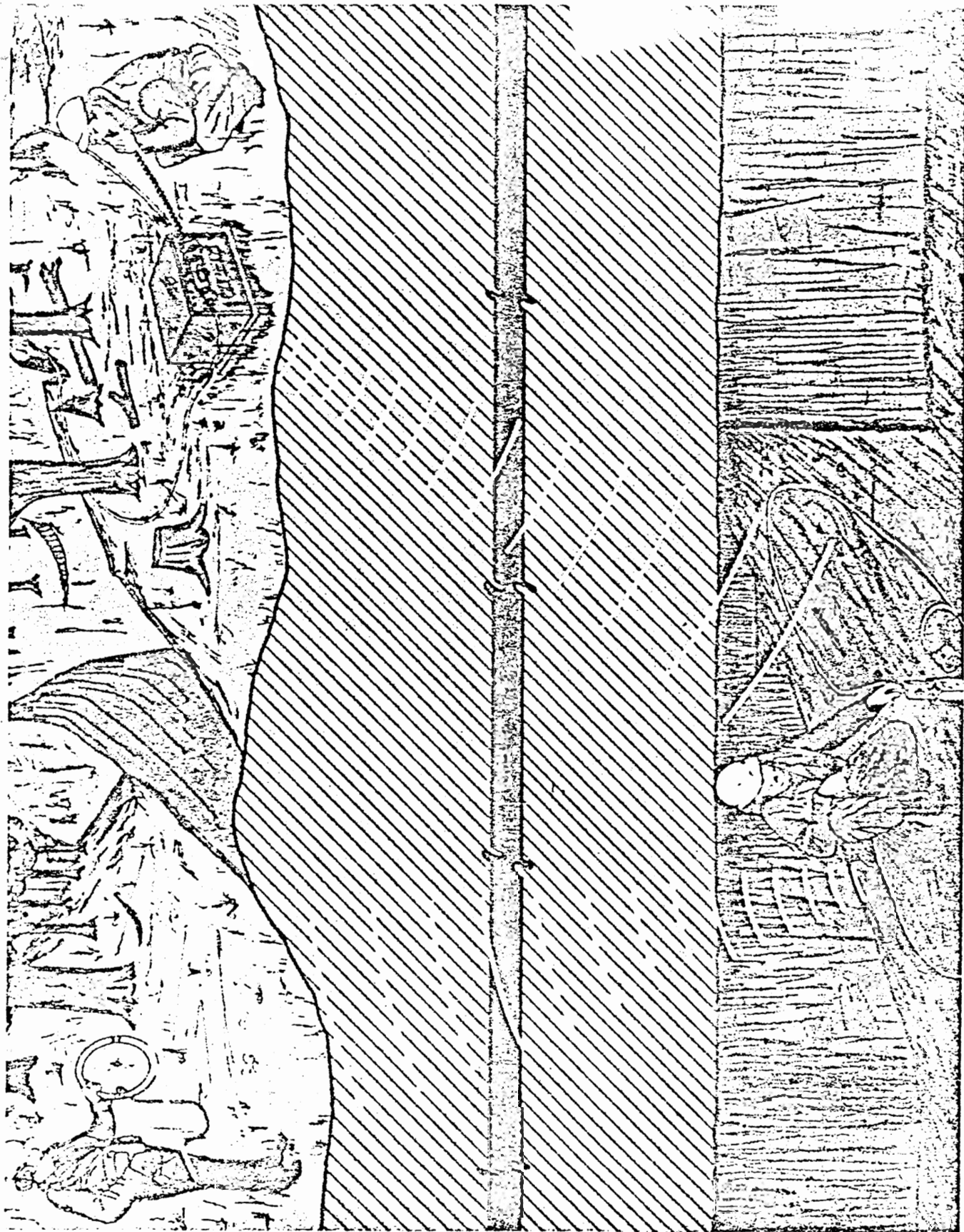


FIGURE 2

51a
ence

(3) The surface above a mine may contain several buildings. While these may be primarily made of nonconductive materials, their presence can hinder the search process, especially if they are directly above the trapped miner.

(4) Various conductive or magnetic structures, including power lines, can also be present. These structures can alter the geometry of the magnetic fields in their vicinity; power lines will produce higher noise levels in their vicinity as well. Thus, if conductive structures or power lines are located directly above the trapped miner, the estimate of his location will probably be less accurate.

(5) The direction of the magnetic-field lines gives an indication of the location of the null. However, automatic interpretation of several such measurements to determine the location of the transmitter is difficult or impossible given an unknown structure of the ground. The electromagnetic direction-finding system requires a search and does not seem to be especially amenable to automation.

A more recent development in the technology for detecting trapped miners from the surface depends upon the accurate measurement of the vector components of electromagnetic (EM) field at various sensor locations on the surface as shown in figure 3 (4). This system uses the same basic transmitter arrangement as EMDF. In an essentially lossless environment, such as in the atmosphere, the transmitter location may be exactly determined by measurement of the propagating EM waves. However, in a conducting medium, such as the earth or water, rapid exponential signal attenuation results from energy dissipated through currents generated in the medium. At lower frequencies, the ability to communicate is better, and this system uses extremely low frequencies (ELF) to propagate an EM wave (2). Measurements are made using at least 2 three-axis field measurement sensors. The report cited, (2) recommends 3 three-axis sensors to avoid "blind spots" and to provide redundancy. This report notes also that background noise affects the magnitude of the field measurements. Simple noise cancellation techniques such as blanking "would seriously hamper the location process, which needs accurate amplitude measurements to achieve an accurate, unambiguous position fix quickly." As a consequence, most of the report discusses signal processing techniques to minimize the deleterious effects of noise on the system. This system will be referred to as the EM field measurement or EMFM system.

As an alternative to these systems, an approach somewhat similar to the EM vector field measurement technique previously described has been proposed. The advantage of this system, illustrated in figure 4, is that it depends only on the phase of the received signal at the sensor locations, so that the effects of attenuation are greatly reduced. The proposed system uses an array of five sensors arranged in a fairly arbitrary, but known through measurement, array on the surface. One sensor is used as a reference, and the remaining four sensors measure the phase difference of arrival (PDOA) with respect to the first sensor.

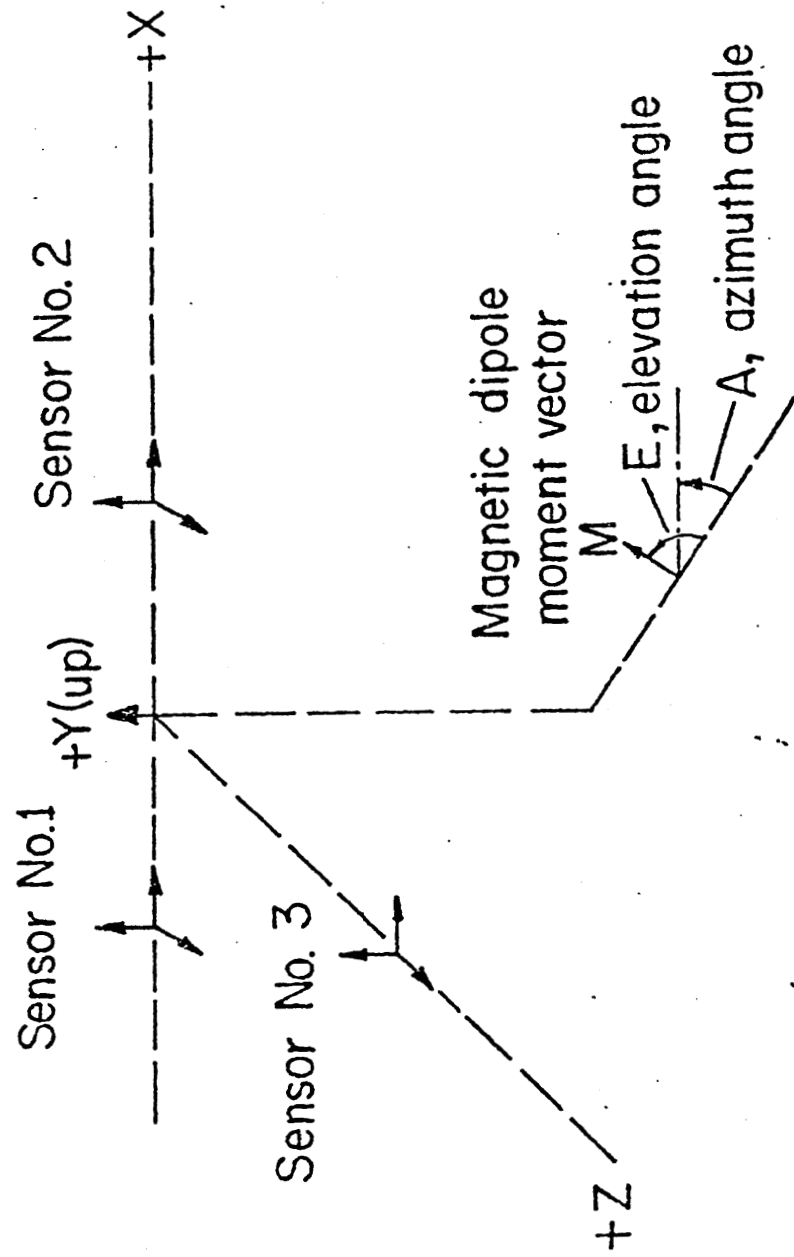


FIGURE 3. - Electromagnetic vector field measurement technique

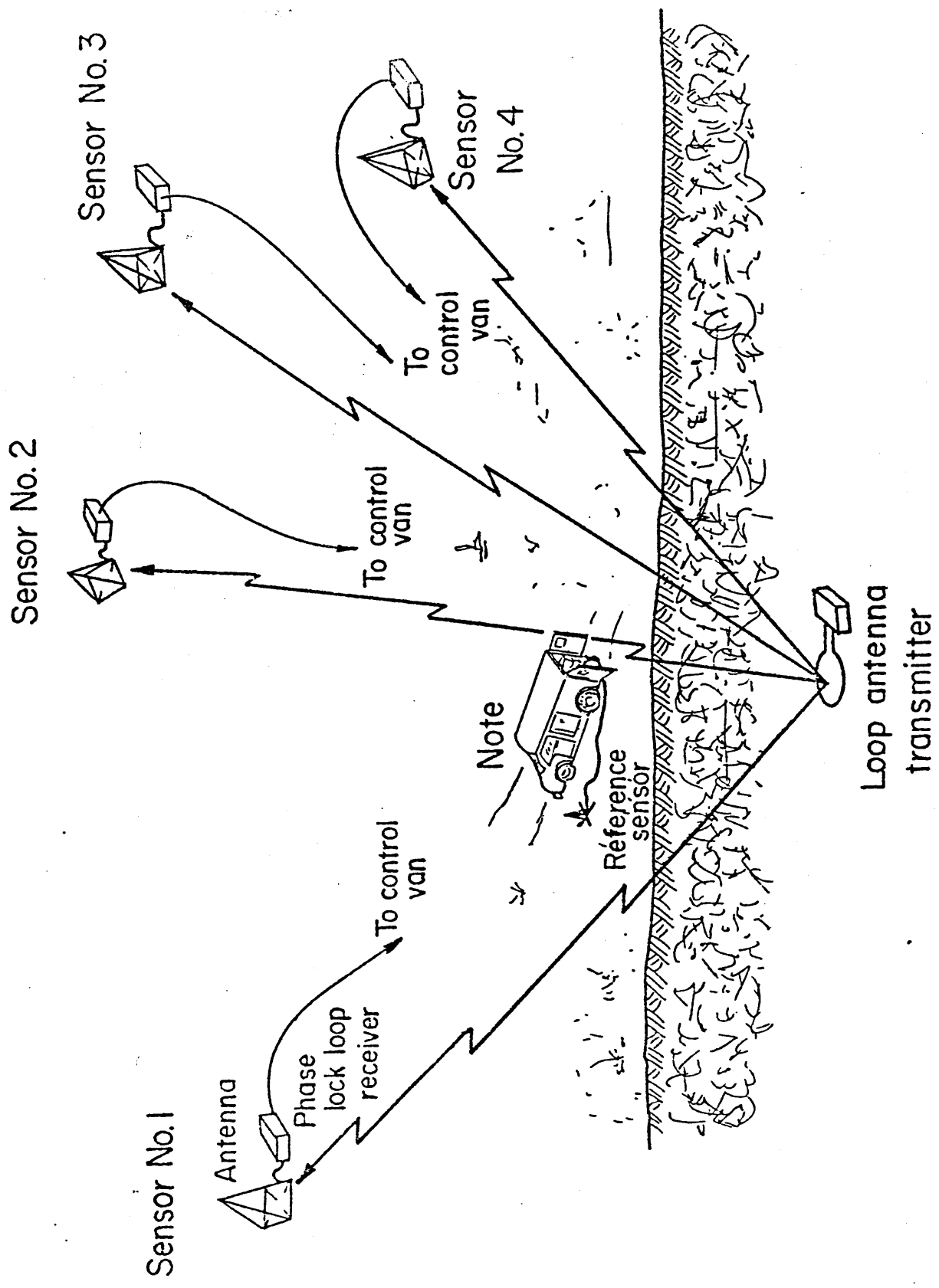


FIGURE 4. - PDOAT system

The communication between sensor positions and reference could be a very high frequency (VHF) link or a dedicated land line. This technique is referred to as the PDOAT. The details of this system are discussed in the following text which illustrates sample calculations.

*** THE PHASE DIFFERENCE OF ARRIVAL TECHNIQUE

One limiting factor in existing transmitter based trapped miner location techniques is the difficulty in obtaining accurate amplitude measurements of the magnetic field. This has led to the development of a technique which depends only on phase measurements. The system would use a computer algorithm to analyze the measured phases of the transmitted signal at multiple receiver locations. This technique assumes a model of the overburden strata as a homogeneous shell of unknown characteristics. As a byproduct of the PDOAT, the average characteristics of the overburden can be determined.

Figure 5 illustrates the arrangement of sensors for implementing the PDOAT. The sensors are at known locations. These may have been previously surveyed or may be determined at the time of deployment of the system. Since it is unlikely that the terrain will be perfectly flat, the sensors are assumed to have coordinates (x_i, y_i, z_i) with respect to any convenient origin, which could be the location of the reference sensor. Thus the reference sensor is assumed at $(0, 0, 0)$ without loss of generality. As figure 5 illustrates, the distance from each sensor, including the reference sensor, to some unknown location (x, y, z) which represents the location of an underground CW transmitter, can then be calculated using analytic geometry. The underground transmitter is assumed to drive a loop antenna which then acts as a magnetic dipole. The same transmitter developed for the EMDF method could be used. As the magnetic field propagates through the overburden, its phase is shifted. The equations which represent this propagation have been documented (7-8), and are included here for completeness. Computer programs to implement the solution to these relationships have also been developed and documented. Thus, referring to figure 5, the following formulation is developed. Considering the loop, whose area x turn product is IA , as a vertical magnetic dipole results in the following magnetic fields in air (i.e. $z > 0$)

$$i\mu_0\omega H_\rho = \frac{\partial^2 F}{\partial \rho \partial z} \quad (1)$$

and

$$i\mu_0\omega H_z = \frac{\partial^2 F}{\partial z^2} \quad (2)$$

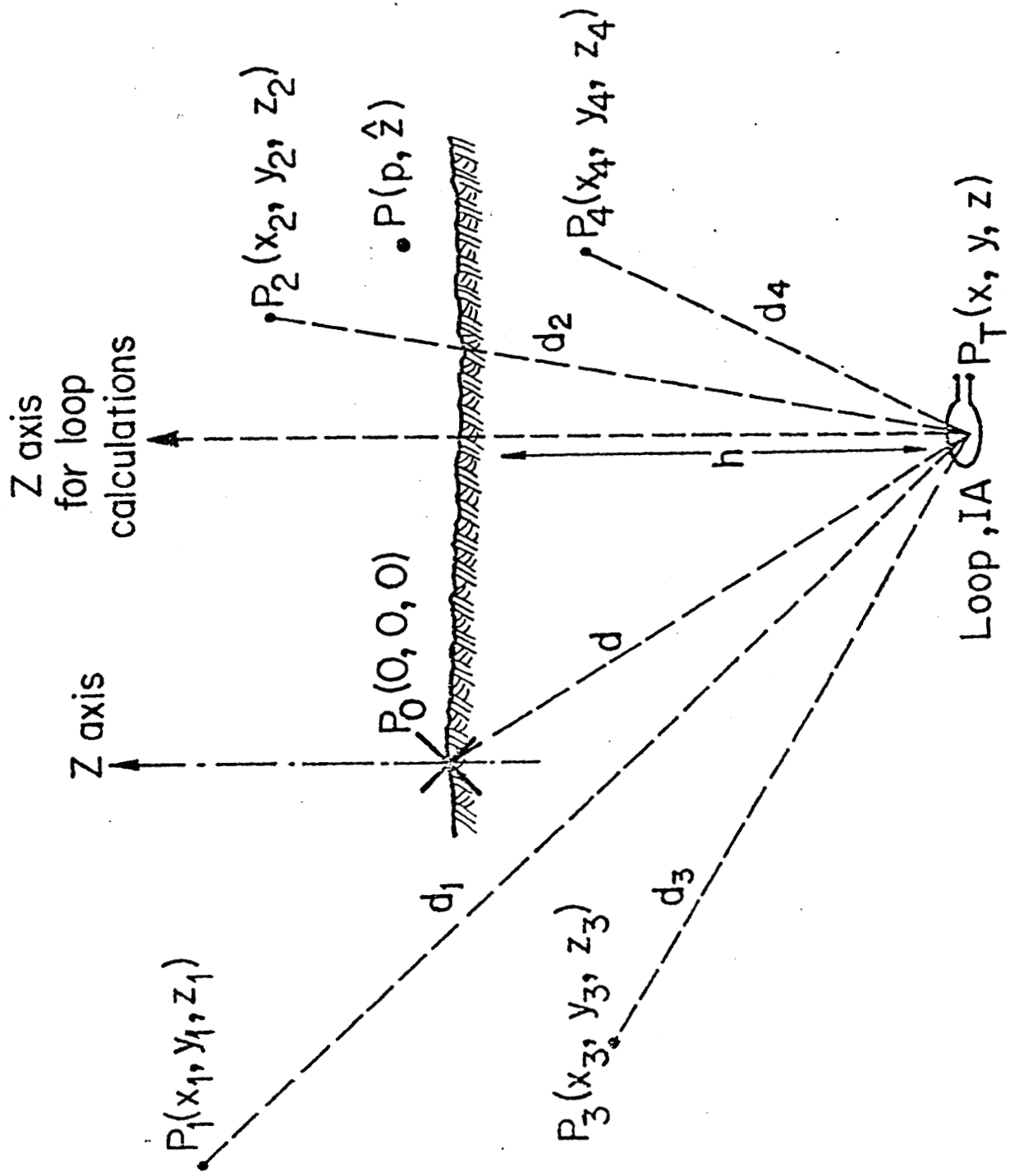


FIGURE 5. - PDOAT array with nomenclature

Where μ_0 is the permeability of free space, ω is the angular frequency, and F is a scalar function. A straightforward boundary analysis leads to the integral form (9):

$$F = \frac{i\mu_0\omega IA}{2\pi} \int_0^\infty \frac{\lambda}{\mu+\lambda} \epsilon^{-\lambda h} J_0(\lambda\rho) d\lambda \quad (3)$$

where $\mu = (\lambda^2 + \gamma^2)$, $\gamma^2 = i\sigma\mu_0\omega$, and J_0 is a Bessel function of order zero. This results in fields at the location (ρ, z) for $z > 0$ of

$$H_\rho = b_0 P \quad (4)$$

and

$$H_z = b_0 Q \quad (5)$$

where

$$P = h^3 \int_0^\infty \frac{\lambda^3}{\lambda+\mu} \epsilon^{-\lambda z} \epsilon^{-\mu h} J_1(\lambda\rho) d\lambda \quad (6)$$

and

$$Q = h^3 \int_0^\infty \frac{\lambda^3}{\lambda+\mu} \epsilon^{-\lambda z} \epsilon^{-\mu h} J_0(\lambda\rho) d\lambda \quad (7)$$

and the normalizing factor is

$$b_0 = \frac{IA}{2\pi h^3} \quad (8)$$

By changing the variable of integration to $x = \lambda h$ the integrals P and Q are expressible in the form

$$P = \int_0^\infty \frac{x^3 \epsilon^{-xz}}{x + (x^2 + iH^2)} \epsilon^{-(x^2 + iH^2)} J_1(xD) dx \quad (9)$$

and

$$Q = \int_0^{\infty} \frac{x^3 \epsilon_{xz}}{x + (x^2 + iH^2)} \epsilon^{-(x^2 + iH^2)} J_0(xD) dx \quad (10)$$

where

$$H = h(\sigma\mu_0\omega)$$

$$D = \rho/h$$

and

$$Z = z/h$$

are dimensionless parameters. These equations are now in a form suitable for numerical integration, and the previously referenced computer program has been prepared to accomplish this task. A listing is given in Appendix A, along with run instructions. Referring again to figure 5, it is seen that

$$d^2 = x^2 + y^2 + z^2 \quad (11)$$

and

$$d_i^2 = (x-x_i)^2 + (y-y_i)^2 + (z-z_i)^2 \text{ for } i = 1 \text{ to } 4 \quad (12)$$

Each d_i can be expressed as $d + \delta_i$, so that δ_i represents the difference between d and d_i . A general equation for the δ_i 's is thus

$$(x-x_i)^2 + (y-y_i)^2 + (z-z_i)^2 = (d+\delta_i)^2 \quad (13)$$

which yields

$$\begin{aligned} x^2 - 2xx_i + x_i^2 + y^2 - 2yy_i + y_i^2 + z^2 - 2zz_i + z_i^2 = \\ d^2 + 2d\delta_i + \delta_i^2 \end{aligned} \quad (14)$$

but since $x^2 + y^2 + z^2 = d^2$, this reduces to

$$2x_ix + 2y_iy + 2z_iz + 2\delta_id + \delta_i^2 = (x_i^2 + y_i^2 + z_i^2) \quad (15)$$

or (for use in the algorithm later)

$$x_ix + y_iy + \delta_id + \delta_i^2 = (x_i^2 + y_i^2 + z_i^2) - zz_i. \quad (16)$$

The relationship between δ_i and Δ_i of the phase sensors at low frequencies of integrals is determined by the characteristics of the overburden, which are unknown. Assuming an average characteristic which is unknown, and relating it to the phase sensor outputs gives a distance increment $\delta_i = k\Delta_i$. Thus, the general equation becomes

$$x_i x + y_i y + kd\Delta_i + .k^2\Delta_i^2 = (x_i^2 + y_i^2 + z_i^2) - zz_i. \quad (17)$$

There are four equations of this type ($i = 1$ to 4), but there are five variables (i.e., x , y , z , k , d). The relationship between x , y , z , and d is however $d^2 = x^2 + y^2 + z^2$. An iterative solution to the equations has been developed and is illustrated in a flow-chart in figure 6. Note that in the special case that all of the sensors are located on a level surface ($z = 0$), the solution is found immediately. In other cases, an initial estimate of z is needed, based on known depths for instance, and the algorithm converges to the required x , y , and z values. A BASIC computer program to perform this algorithm on the Tektronix 4052 microcomputer has been used successfully to implement this method. A listing of this program is given in Appendix B.

In order to implement the system in real hardware, it is necessary to determine a reasonable word size for the A/D converter which will provide the phase information for the computer. Assuming a phase measuring accuracy of 0.02 degrees, the radial accuracy is $0.02 \times \pi / 180 = 0.349 \times 10^{-3}$ radian.

A reasonable choice for the A/D converter is 12 bits which will provide 4096 levels of quantized output. Thus, the accuracy of measurement at different frequencies and values of conductance can be estimated from the relationship $bd = WR$.

TABLE 1. - Estimated position resolution, m

Conductivity	Frequency, Hz			
	100	200	1,000	2,000
$s = 10^{-2}$	0.176	0.124	0.056	0.039
$s = 10^{-3}$.538	.380	.170	.120
$s = 10^{-4}$	1.76	1.245	.556	.394

⁴Reference to specific brand or trade names is made for identification only and endorsement by the Bureau of Mines is not implied.

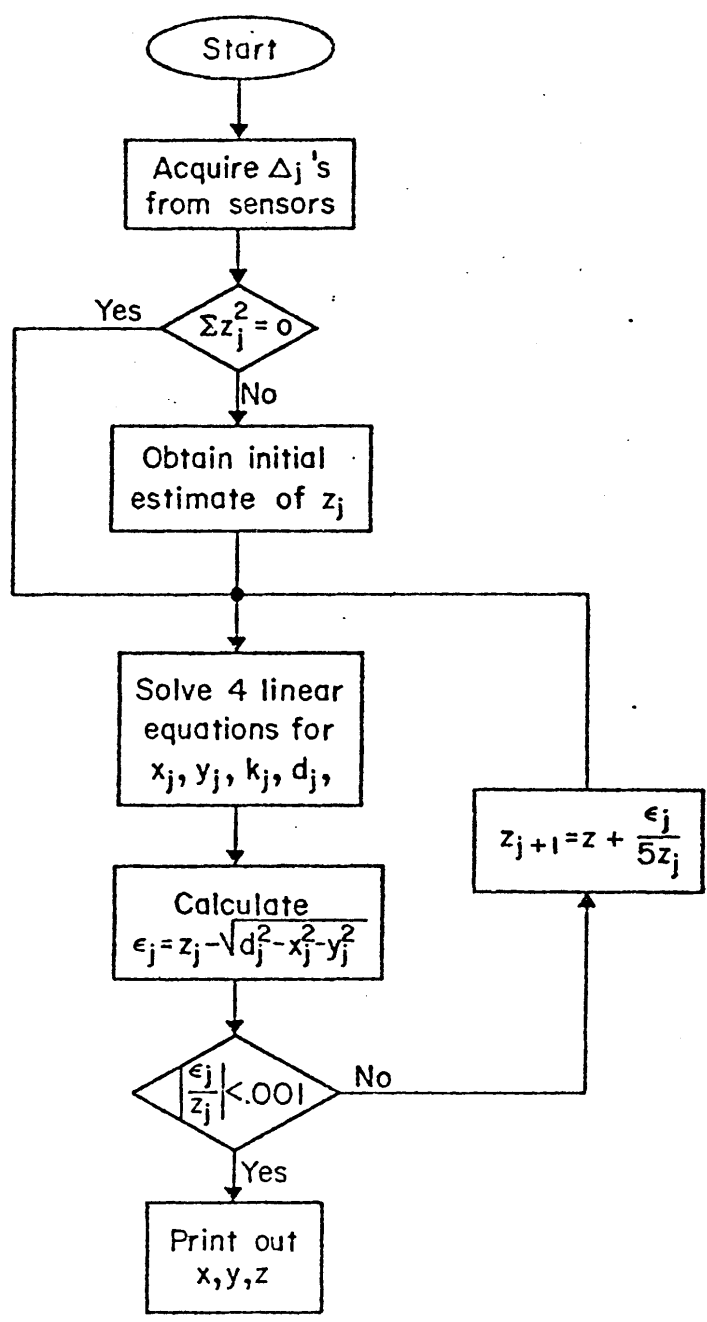


FIGURE 6. - Flow chart of PDOAT algorithm

Since β is inversely proportional to $\sqrt{f\sigma}$, it can be seen that

resolution of position increased with \sqrt{f} as well as $\sqrt{\sigma}$. Of course, σ is an assumed constant parameter of the overburden, but frequency is a design parameter of the system. In order to provide adequate resolution but to avoid the higher frequency attenuation effects, a frequency range of 100 to 1,000 Hz seems satisfactory. Calculations based on some typical values are presented in the following sample problem using PDOAT.

*** SAMPLE CALCULATIONS USING PDOAT

Assume that the PDOAT system has been set up using 12 bit A/D convertors (approximately range -30° to $+30^\circ$) and the sensor sites have been determined relative to the reference site. These measurements are assumed to have been in meters.

TABLE 2. - Sensor coordinates

Station	Distance, m		
	x	y	z
Sensor:			
1.....	20	25	5
2.....	-15	30	0
3.....	-20	-30	2
4.....	25	-25	-1

Assume further that the transmitter of the trapped miner is at 30, 40, and 200 m and that the constant related to the overburden and frequency is 1,000 (which is roughly the value at 200 Hz with $\sigma = 10^{-3}$).

Then the δ_i 's defined in the previous chapter can be found, as well as the corresponding Δ_i 's. Thus:

$$d^2 = 30^2 + 40^2 + 200^2 = 42500; \quad d = 206.155$$

$$d_1^2 = 10^2 + 15^2 + 195^2 = 38350; \quad d_1 = 195.832$$

$$d_2^2 = 45^2 + 10^2 + 200^2 = 42125; \quad d_2 = 205.244$$

$$d_3^2 = 50^2 + 70^2 + 198^2 = 46604; \quad d_3 = 215.880$$

$$d_4^2 = 5^2 + 65^2 + 201^2 = 46651; \quad d_4 = 211.308$$

$$\delta_1 = d_1 - d = -10.323; \quad \Delta_1 = -0.010323$$

$$\delta_2 = d_2 - d = -0.911; \quad \Delta_2 = -0.000911$$

$$\delta_3 = d_3 - d = 9.725; \quad \Delta_3 = 0.009725$$

$$\delta_4 = d_4 - d = 5.153; \quad \Delta_4 = 0.005153$$

Since the Δ_1 's will be quantitized and subject to error, the quantitized values will be ($q = 0.00025$)

$$\Delta_1' = -0.01025; \Delta_2' = -0.00100; \Delta_3' = 0.00975; \Delta_4' = 0.00525.$$

These values were used as the inputs to the proposed PDOAT system program. The results as obtained from the Tektronix 4052 are as follows:

X =	29.414451706	K =	1012.65790474
Y =	40.3003627847	D =	203.234325237
Z =	196.970505922		

The program was also run with a greater error criterion in line 410, with no appreciable change in results. The unquantitized phase variables were also input and the results converged to the expected values with errors of less than 0.01 percent.

*** DEVELOPMENT OF THE PDOAT SYSTEM

In order to test the PDOAT concept in an actual mine environment, a series of field tests were designed and carried out. Since the Bureau (3) had previously developed a suitable transmitter, a test unit was obtained. The unit was built by Collins Radio Group and identified as PN 622-2622-051, Serial No. 1. The transmission frequency of this unit is 3,030 Hz. This transmitter is designed to snap onto a miner's cap lamp battery and is coupled to an antenna consisting of one loop of AWG #18 wire wrapped around a coal pillar (length about 85 m).

For a first test, a simple antenna and tuned circuit receiver system was built. A block diagram of this system is shown in figure 7. Figure 8 shows a schematic of the input amplifier section and figure 9 shows a schematic of the narrow band amplifier. The antenna consists of 2,500 turns of AWG #34 enamelled wire wound on a 64 cm diameter. The cross section of the antenna is approximately 2- by 2-cm. The antenna has a resistance of 4,500 Ω and a computed inductance of approximately 8 henries. A Faraday shield consisting of two layers of aluminum foil covers the coil winding and is grounded to the receiver chassis during operation. The receiver uses a balanced high-input impedance, low noise amplifier circuit, followed by two stages of narrow band amplification consisting of 741 op-amps with twin-tee feedback networks. Each narrow band stage is followed by a high input impedance stage to prevent loading of the tuned circuits. The output consists of four stages of high gain amplification. The last two can be bypassed if less gain is needed. Low and high frequency rolloff is provided to help reject power line and radio frequency interference.

This system was successfully deployed on June 2, 1982, at North River Energy Corporation's No. 1 Mine near Berry, AL. The approximate depth of the transmitter was 167 m. A strong signal was detected at several surface locations. Figure 10 shows the system components. Figure 11 shows the system during the test.

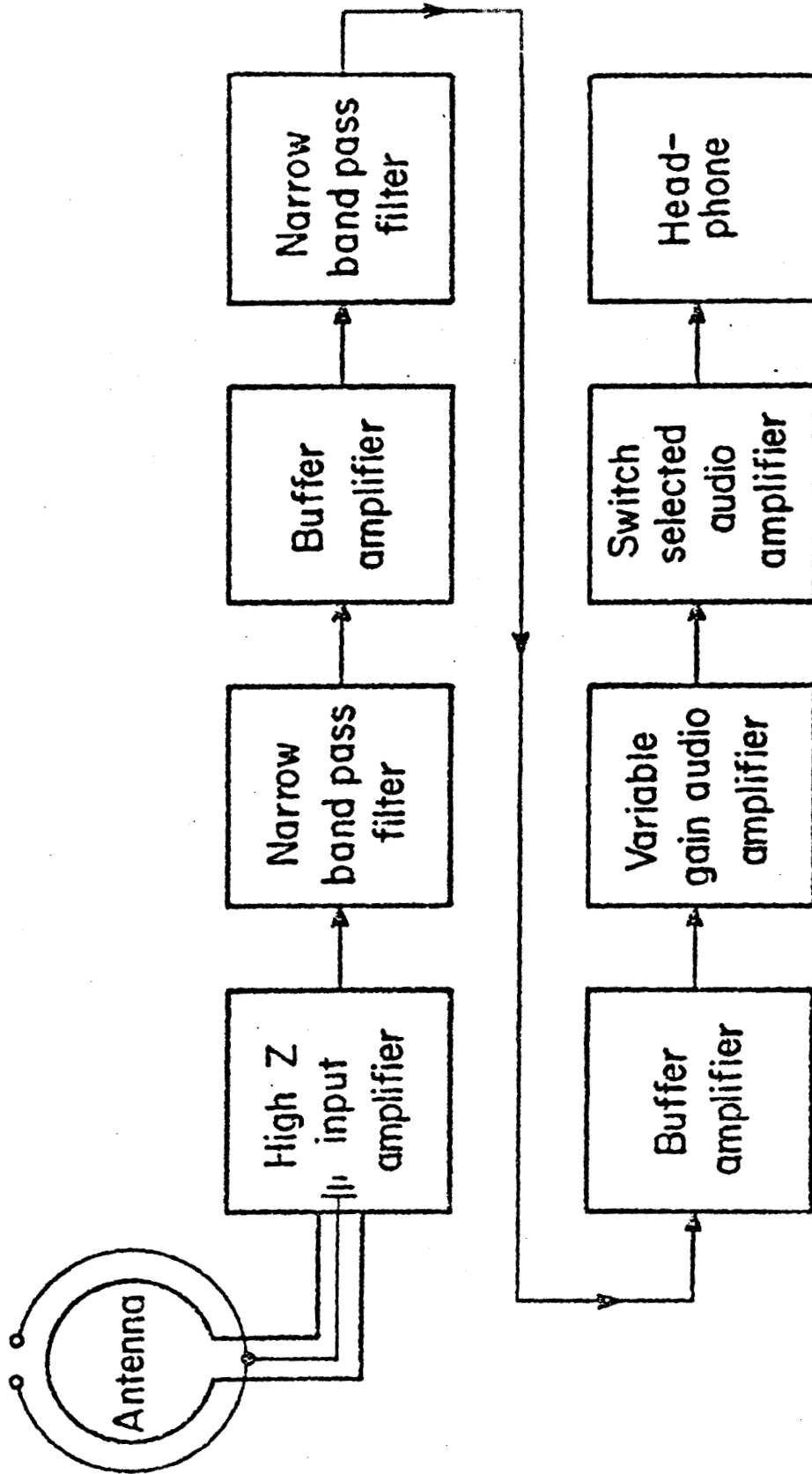


FIGURE 7. - Block diagram of preliminary PDOAT receiver

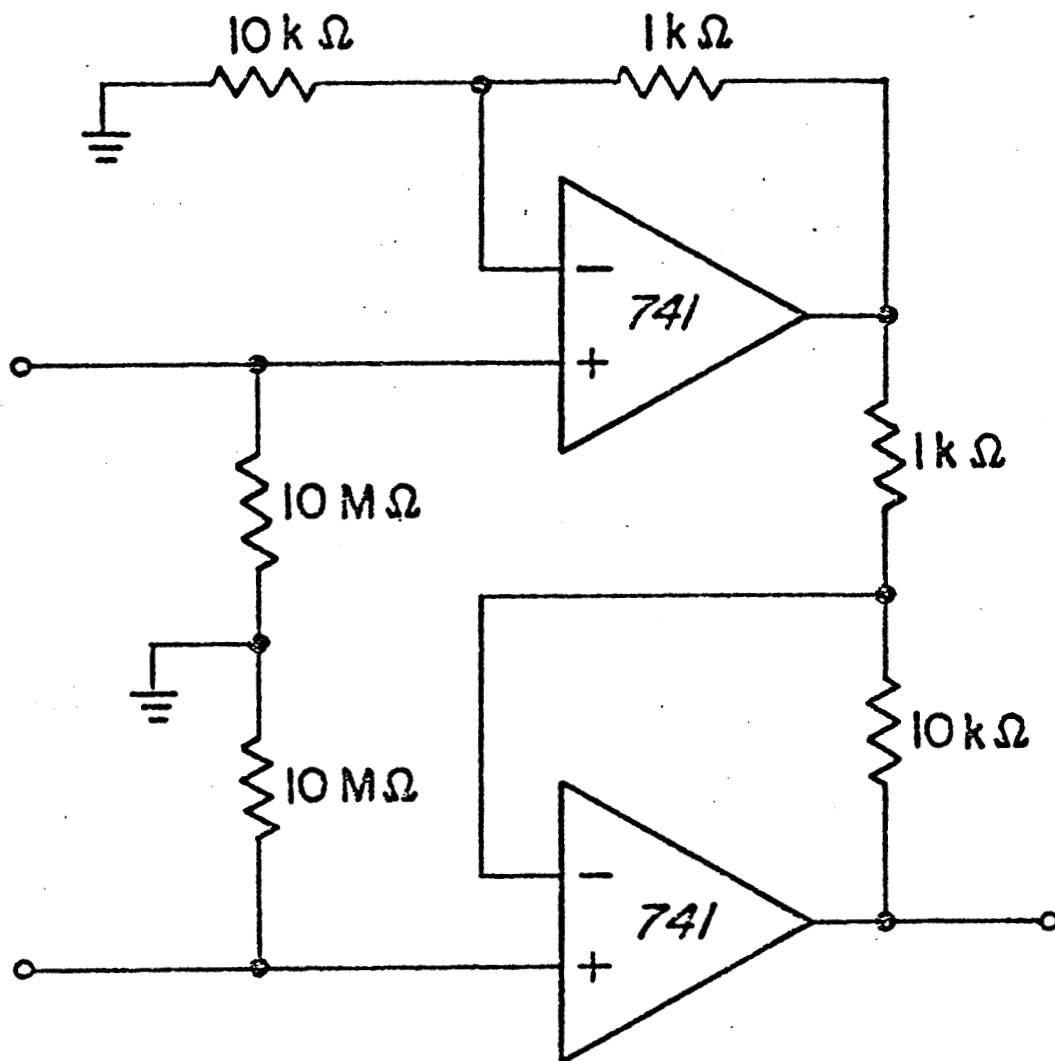


FIGURE 8. - Schematic diagram of high-impedance balanced input amplifier

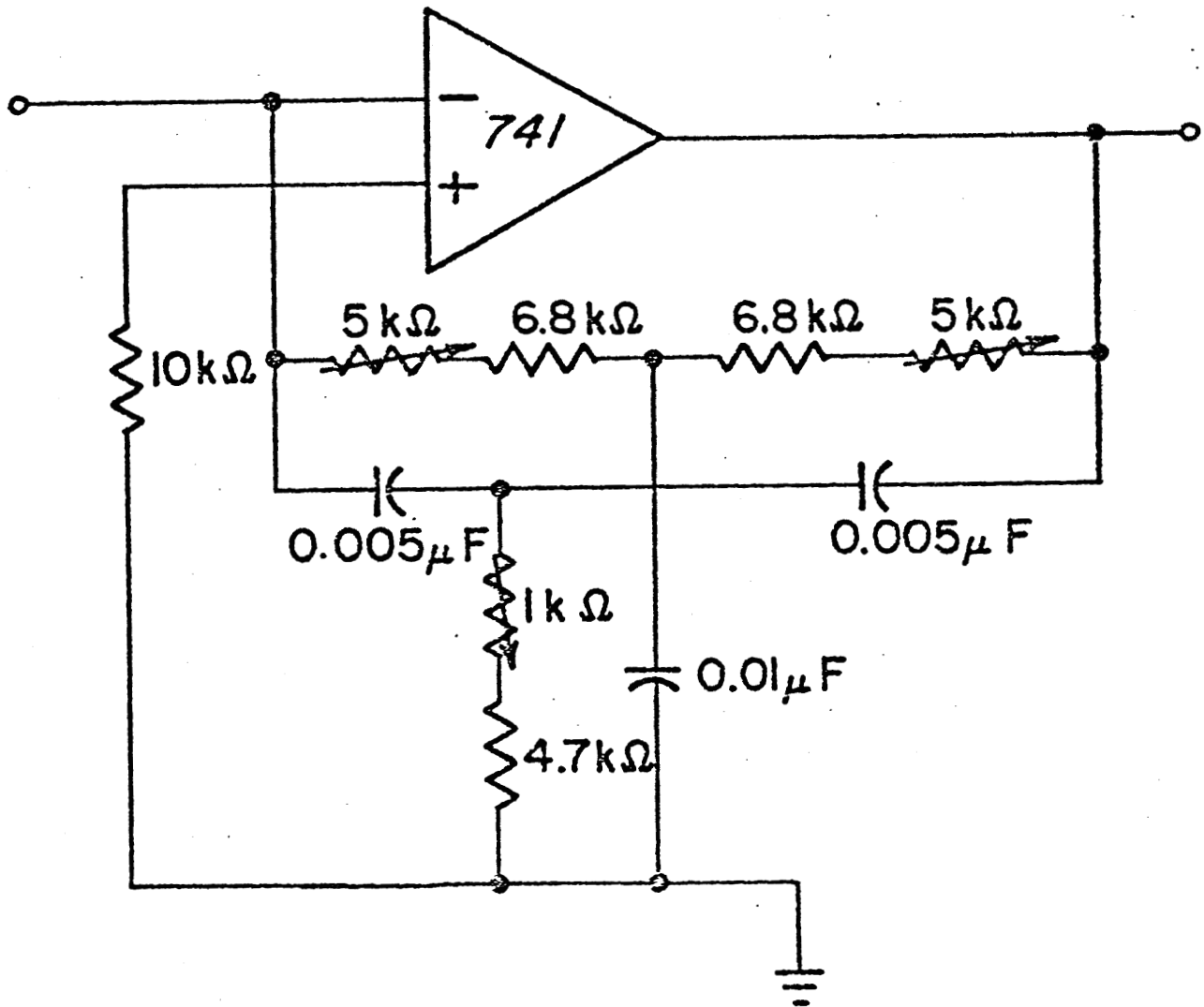


FIGURE 9. - Schematic diagram of narrow band-pass filter using twin-tee feedback

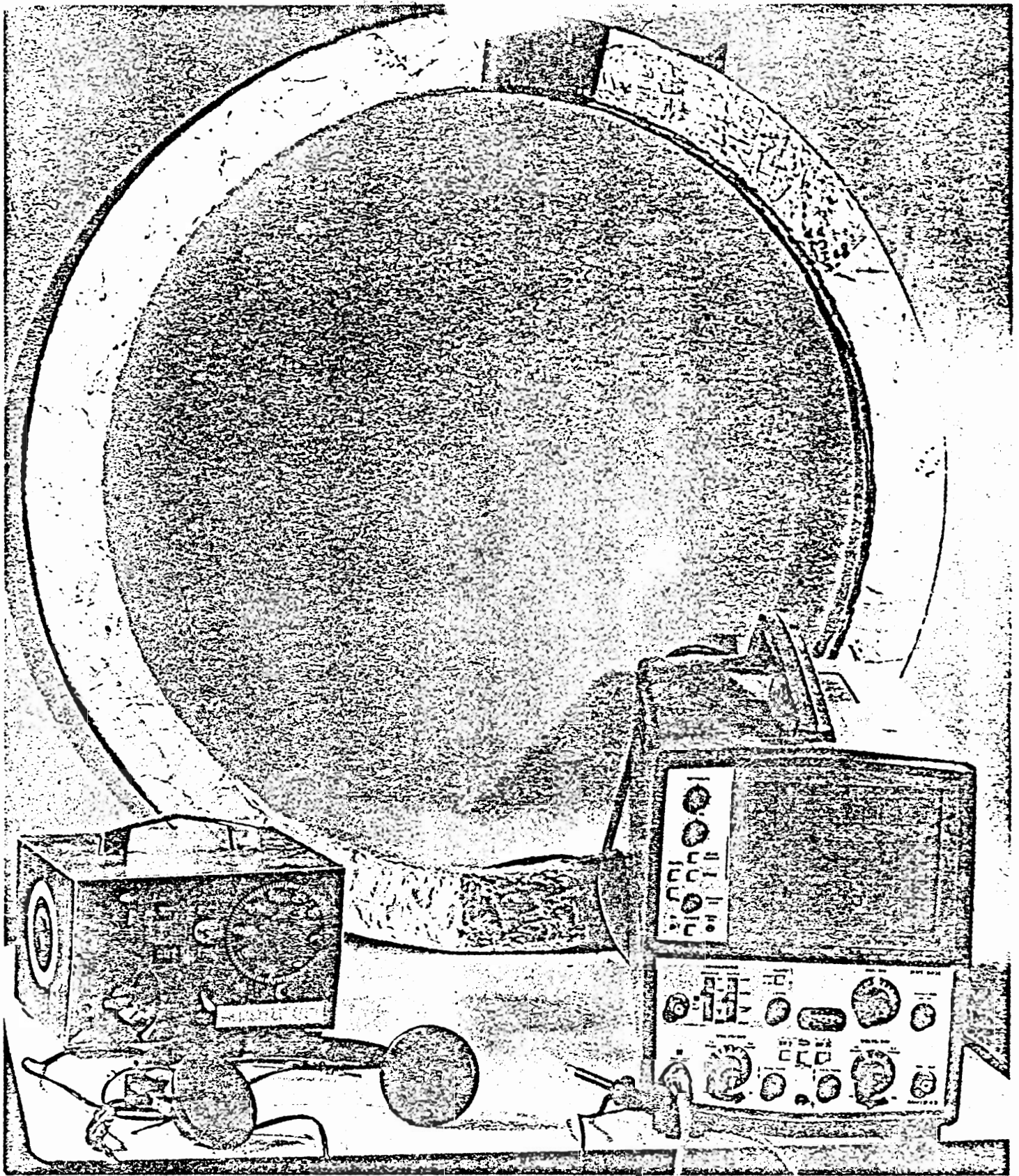


FIGURE 10. - Photograph of PDOAT system components

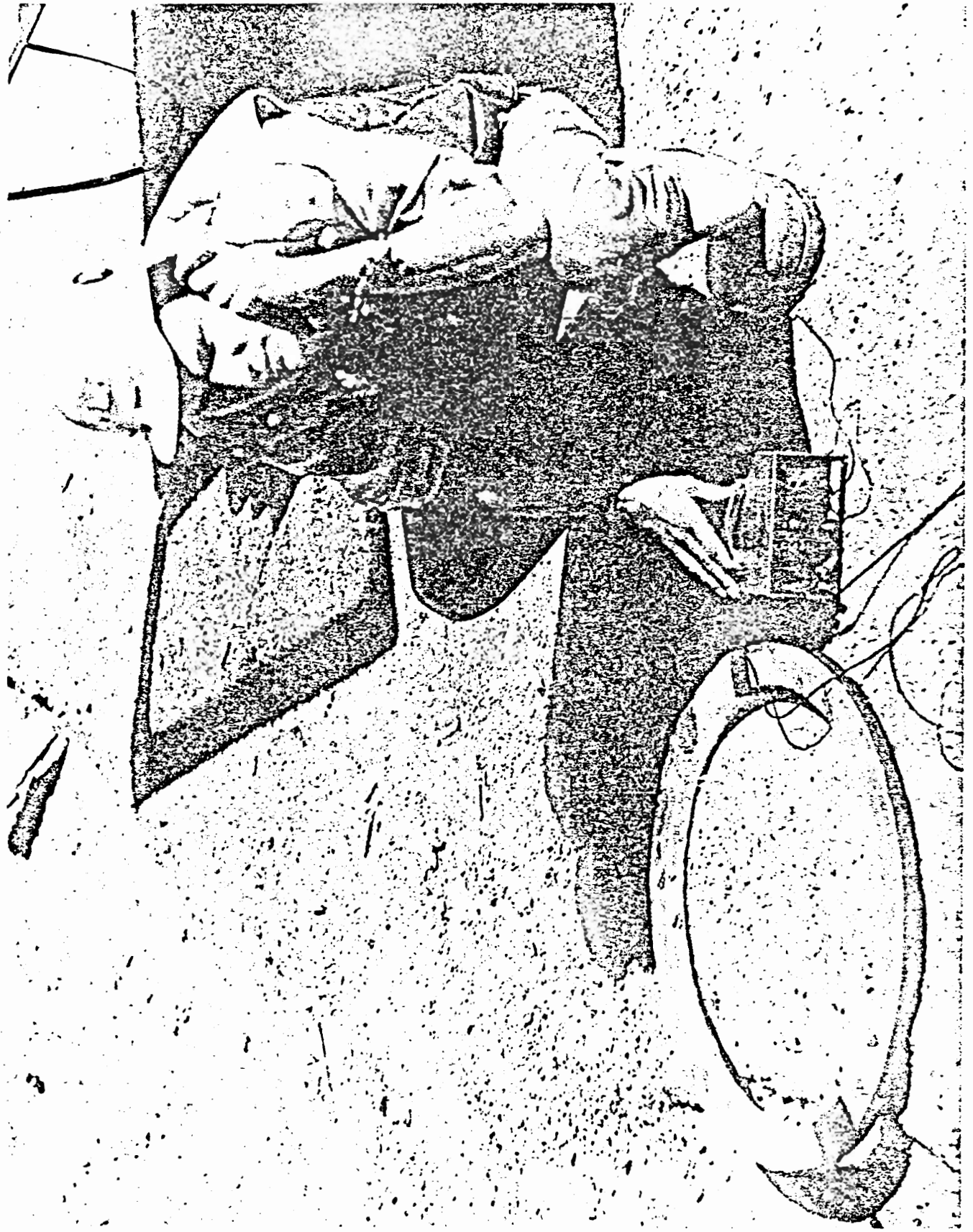


FIGURE 11. - Photograph of USBM personnel deploying PDOAT receiver

After determining that the signal was readily detectable from the surface, a more elaborate test was devised. For this test, a phase-lock-loop (PLL) chip was added to the previously designed circuit. A block diagram of this receiving system is shown in figure 12. Using the previously designed front end, the filtered signal was fed into a phase detector and the PLL chip was used to determine the relative phase of the received signal. A Tektronix oscilloscope, model T-912, was used to observe the received signal. The output of the PLL was suitable for application to the A/D converter in the Tektronix 4052 and the previously described algorithm then could calculate the location of the transmitter.

**** RECOMMENDATIONS

The review of existing and developing techniques in this report indicates various restrictions and expectations that must be reconciled. Primary items of interest are cost, complexity, and accuracy.

The relatively low cost and simplicity of the EMDF system lends itself to rapid deployment in case of an emergency. However, the less sophisticated "null-seeking" method may impose severe limitations in its use. In some cases, it may not be possible or feasible to actually traverse the entire cross section of a mine in order to find a null. The EMFM and PDOAT systems share the advantage that once deployed, no further excursions are required to seek the transmitter location. The primary disadvantage of the EMFM system is its reliance on accurate field strength measurements. The primary reason for its complex digital processing is to counteract degradation of the signal used for this measurement. The PDOAT system, on the other hand, relies entirely on phase measurements. The strength of the signal needs only to be strong enough to allow the phase lock loops in the sensors to lock in.

Further research with the PDOAT is required and should include design and deployment of the antenna array system coupled with the microcomputer and appropriate software to determine system performance. In addition, extensive field testing should be conducted.

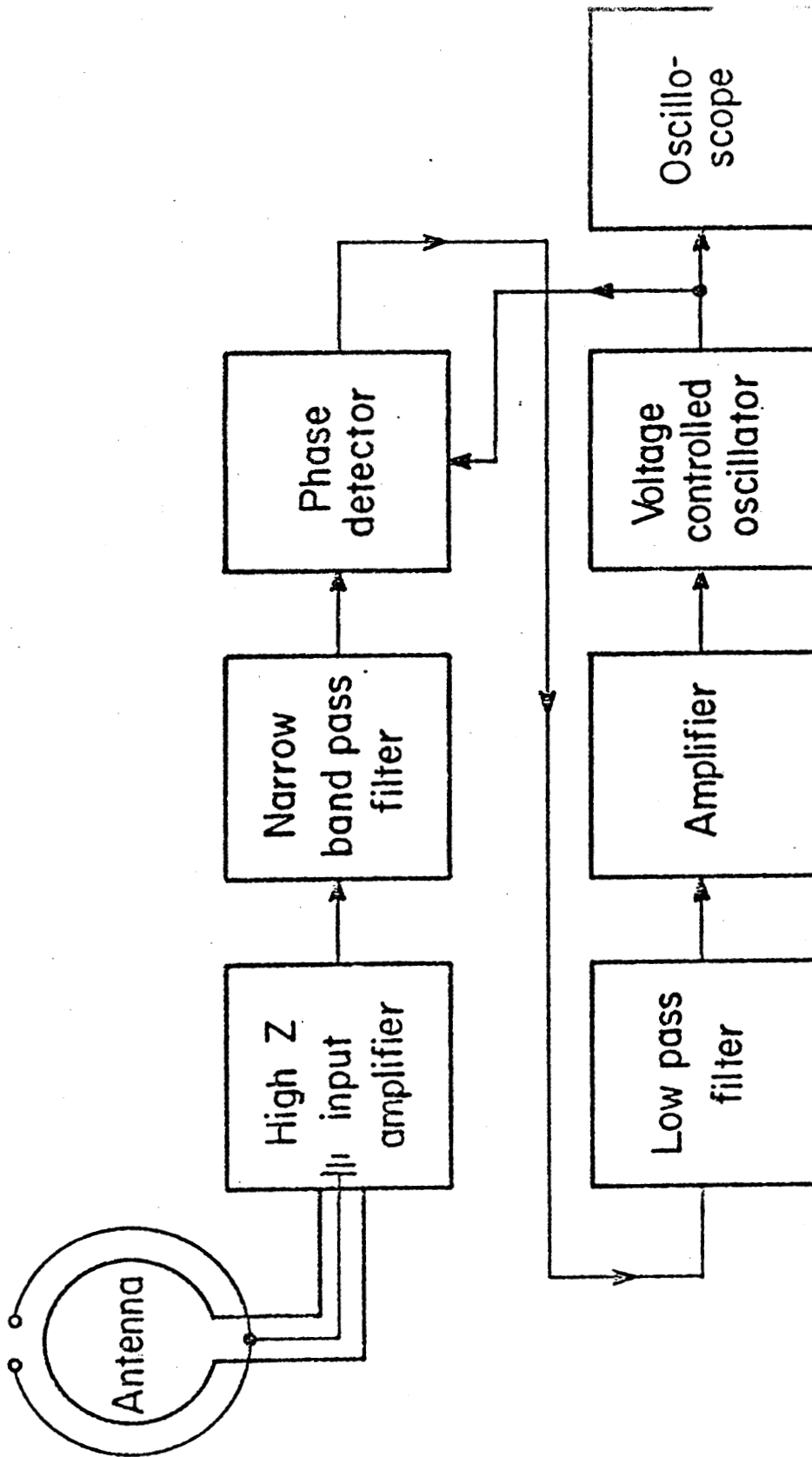


FIGURE 12. - Block diagram of phase-locked loop receiver

REFERENCES

1. Duda, S. J. Trapped Miner Location and Communication System Development Program, v. II: Detection and Location of Entrapped Miners by Seismic Means: Methods and Computer Programs. Westinghouse Electric Corp., Baltimore, MD; BuMines OFR 41(2)-74, May 1973, 64 pp., NTIS, PB-235 606.
2. Kraichman, M. B. Handbook of Electromagnetic Propagation in Conducting Media, NAVMAT P-2302, U.S. Government Printing Office, 1970, p. 2302.
3. Powell, J. A. An Electromagnetic System for Detecting and Locating Trapped Miners. BuMines RI 8159, 1976, p. 15.
4. Rorden, L. H., T. C. Moore, E. C. Fraser, and L. R. Bulduc. Development of Systems Concept for Location of Trapped Miners in Deep Mines by an Electromagnetic Method. Phase 1 Report, Contract No. JO199009, Develco, Inc., Sunnyvale, CA, Oct., 1979, 119 pp.
5. Sacks, H. K. Trapped-Miner Location and Communication Systems. Underground Mine Communications, Part 4, Section-to-Place Communications, BuMines IC 8745, 1977, p. 80.
6. U.S. Bureau of Mines. Seismic System for Detecting and Locating Trapped Miners. Technology News No. 100, Bureau of Mines, May, 1981.
7. Wait, J. R. Electromagnetic Induction Technique for Locating a Buried Source. IEEE Transactions on Geoscience Electronics. v. GE-9, No 2, April, 1971, pp. 95-98.
8. _____. Criteria for Locating an Oscillating Magnetic Dipole Buried in the Earth. Proc. of IEEE, June, 1971, pp. 1033-1035.
9. Wait, J. R. Electromagnetic Fields of Sources in Lossy Media. Antenna Theory, Pt. II. R. E. Collins and F. J. Zucker, (ed). McGraw-Hill, New York, 1969, Ch. 24, pp. 468-471.

LIST OF ILLUSTRATIONS

1. Seismic system.....
2. Electromagnetic direction-finding system.....
3. Electromagnetic vector field measurement technique.....
4. PDOAT system.....
5. PDOAT array with nomenclature.....
6. Flow chart of PDOAT algorithm.....
7. Block diagram of preliminary PDOAT receiver.....
8. Schematic diagram of high-impedance balanced input amplifier.....
9. Schematic diagram of narrow band-pass filter using twin-tee feedback.....
10. Photograph of PDOAT system components.....
11. Photograph of USBM personnel depolying PDOAT receiver...
12. Block diagram of phase-lock loop receiver.....

Appendix A. - Fortran program for estimating phase angle through overburden

```

1:      COMPLEX PX, PY, PZ, PR, PPHI
2:      IN=5
3:      PI=3.1415926536
4:      DTR=PI/180.
5:      NDS=1
6:      H=.05
7:      Z=0.0
8:      S=.03
9:      YL=.6
10:     PHI=0.0
11:     DR=.05
12:     NR=20
13:     PRINT 40
14:40   FORMAT ('1H,Z,S,L,PHI')
15:     PRINT 50,H,Z,S,YL,PHI
16:50   FORMAT(' H=',F8.5,' Z=',F6.2,' S=',F6.2,' YL=',F9.4,' PHI=',F9.4)
17:     PHIR=PHI*DTR
18:     CP=COS(PHIR)
19:     SP=SIN(PHIR)
20:     PRINT 70
21:70   FORMAT (' R,PZMAG,PRMAG,PPHIMAG,PZPH,PRPH,PPHIPH')
22:     DO 60 J=1,NR
23:     R=DR*(J-1)
24:     X=R*CP
25:     XD=ABS(X-S)
26:     IF (XD-1.E-4) 80,80,90
27:80    R=R+.1*DR
28:     X=R*CP
29:90    Y=R*SP
30:     YD=ABS(Y-YL)
31:     IF (YD-1.E-4) 100,100,110
32:100   R=R+.1*DR
33:     X=R*CP
34:     Y=R*SP
35:110  CALL PINT(H,Z,X,S,Y,YL,PX,PY,PZ)
36:     PR=PX*CP+PY*SP
37:     PPHI=PY*CP-PX*SP
38:     PZM=CABS(PZ)
39:     PRM=CABS(PR)
40:     PPHIM=CABS(PPHI)
41:     PZP=CANG(PZ)/DTR
42:     PRP=CANG(PR)/DTR
43:     PPHIP=CANG(PPHI)/DTR
44:60   PRINT 130,R,PZM,PRM,PPHIM,PZP,PRP,PPHIP
45:130  FORMAT (E14.4,6E16.5)
46:20   CONTINUE
47:     END
48:     SUBROUTINE PINT(H,Z,X,S,Y,YL,PX,PY,PZ)
49:     COMPLEX CI,PXI,PYI,PZI,RAD,T,FAC,PX,PY,PZ
50:     GMAX=(12.+H)/(1.+Z)
51:     RMAXI=1./SQRT((X+S)**2+(Y+YL)**2)

```

```

52:      RMAXI=5) 20,10,10
53:20    NH=GMAX/(2-RMAXI)
54:      GO TO 30
55:10    NH=GMAX
56:30    NI=2*NH+2
57:      DG=GMAX/NI
58:      CI=(0.,1.)
59:      H2=H*H
60:      PXI=(0.,0.)
61:      PYI=(0.,0.)
62:      PZI=(0.,0.)
63:      DO 40 I=1,NI
64:        G=DG*I
65:        IF (I-NI) 50,60,60
66:60    CF=1.
67:      GO TO 70
68:50    CF=3.+(-1.)**I
69:70    G2=G*G
70:      RAD=CSQRT(G2+CI*H2)
71:      T=G*CEXP(-RAD)/(G+RAD)
72:      FAC=G2*T*EXP(-G*Z)
73:      CALL FXINT(G,X,S,Y,YL,FX)
74:      CALL FYINT(G,X,S,Y,YL,FY)
75:      CALL FINT(G,X,S,Y,YL,FZ)
76:      PXI=PXI+FAC*FX*CF
77:      PYI=PYI+FAC*FY*CF
78:40    PZI=PZI+FAC*FZ*CF
79:      PX=PXI*DG/3.
80:      PY=PYI*DG/3.
81:      PZ=PZI*DG/3.
82:      RETURN
83:      END
84:      SUBROUTINE FINT(G,X,S,Y,YL,F)
85:      IF (S-YL) 10,20,20
86:20    N=G*S
87:      GO TO 30
88:10    N=G*YL
89:30    NI=2*N+11
90:      RNP=YL-Y
91:      RNN=-YL-Y
92:      RDP=S-X
93:      RDN=-S-X
94:      TH1=ATAN2(RNP,RDP)
95:      TH2=ATAN2(RNP,RDN)
96:      TH3=ATAN2(RNN,RDN)
97:      TH4=ATAN2(RNN,RDP)
98:      DT1=(TH2-TH1)/(NI-1)
99:      IF (YL-Y) 32,32,34
100:32   DT2=(TH3-TH2)/(NI-1)
101:      GO TO 37
102:34   DT2=(TH3-TH2+6.2831853072)/(NI-1)
103:36   IF (X-S) 37,37,38
104:38   DT4=(TH1-TH4-6.2831853072)/(NI-1)
105:      GO TO 39
106:37   DT4=(TH1-TH4)/(NI-1)
107:39   DT3=(TH4-TH3)/(NI-1)
108:      A=4.*G*S*YL

```

```

109:      T11=0.
110:      T12=0.
111:      T13=0.
112:      T14=0.
113:      DO 15 I=1,NI
114:      IF (I-1) 40,40,50
115:40     CF=1.
116:      GO TO 60
117:50     IF (I-NI) 70,40,40
118:70     CF=3.+(-1.)**I
119:60     T1=TH1+DT1*(I-1)
120:      T2=TH2+DT2*(I-1)
121:      T3=TH3+DT3*(I-1)
122:      T4=TH4+DT4*(I-1)
123:      R=RNP/SIN(T1)
124:      CALL FJI(G,R,TT)
125:      T11=T11+TT*CF
126:      R=RDN/COS(T2)
127:      CALL FJI(G,R,TT)
128:      T12=T12+TT*CF
129:      R=RNN/SIN(T3)
130:      CALL FJI(G,R,TT)
131:      T13=T13+TT*CF
132:      R=RDP/COS(T4)
133:      CALL FJI(G,R,TT)
134:15     T14=T14+TT*CF
135:      F=(T11*DT1+T12*DT2+T13*DT3+T14*DT4)/(3.*A)
136:      RETURN
137:      END
138:      SUBROUTINE FJI(G,R,P)
139:      ARG=G*R
140:      CALL J1X(ARG,B1)
141:      P=B1*R
142:      RETURN
143:      END
144:      SUBROUTINE FXINT(G,X,S,Y,YL,FX)
145:      N=G*YL
146:      NI=2*N+5
147:      DY=YL/(N+2)
148:      A=4.*G*S*YL
149:      FXI=0.
150:      DO 10 I=1,NI
151:      IF (I-1) 20,20,30
152:20     CF=1.
153:      GO TO 40
154:30     IF (NI-I) 20,20,50
155:50     CF=3.+(-1.)**I
156:40     YP=-YL+DY*(I-1)
157:      CALL FXJI(G,X,S,Y,YP,DIF)
158:      TX=DIF*CF
159:10     FXI=FXI+TX
160:      FX=FXI*DY/(3.*A)
161:      RETURN
162:      END
163:      SUBROUTINE FYINT(G,X,S,Y,YL,FY)
164:      N=G*S
165:      NI=2*N+5

```



```

166:      DX=PS/(N+2)
167:      A=4.*G*S*YL
168:      FYI=0.
169:      LO 10 I=1,N1
170:      IF (I-1) 20,20,30
171:20    CF=1.
172:      GO TO 40
173:30    IF (NI-I) 20,20,50
174:50    CF=3.+(-1.)**I
175:40    XP=-S+DX*(I-1)
176:      CALL FYJI(G,Y,YL,X,XP,DIF)
177:      TY=DIF*CF
178:10    FYI=FYI+TY
179:      FY=FYI*DX/(3.*A)
180:      RETURN
181:      END
182:      SUBROUTINE FxJI(G,X,S,Y,YP,DIF)
183:      XD2=(X-S)**2
184:      YD2=(Y-YP)**2
185:      R=SQRT(XD2+YD2)
186:      ARG=G*R
187:      CALL JOX(ARG,BD)
188:      XS2=(X+S)**2
189:      R=SQRT(XS2+YD2)
190:      ARG=G*R
191:      CALL JOX(ARG,BS)
192:      DIF=BD-BS
193:      RETURN
194:      END
195:      SUBROUTINE FYJI(G,Y,YL,X,XP,DIF)
196:      YD2=(Y-YL)**2
197:      XD2=(X-XP)**2
198:      R=SQRT(XD2+YD2)
199:      ARG=G*R
200:      CALL JOX(ARG,BD)
201:      YS2=(Y+YL)**2
202:      R=SQRT(XD2+YS2)
203:      ARG=G*R
204:      CALL JOX(ARG,BS)
205:      DIF=BD-BS
206:      RETURN
207:      END
208:      FUNCTION CANG(Z)
209:      COMPLEX Z
210:      ZM=CABS(Z)
211:      IF (ZM) 10,10,20
212:20    X=REAL(Z)
213:      Y=AIMAG(Z)
214:      CANG=ATAN2(Y,X)
215:      GO TO 30
216:10    CANG=0.
217:30    RETURN
218:      END
219:      SUBROUTINE JOX(X,BJZERO)
220:      IF (X) 5,10,15
221:5      AX=-X
222:      GO TO 20

```

```

223:10      BJJZERO=0.0
224:        RETURN
225:15      AX=X
226:20      IF (AX-4.0) 25,25,30
227:25      T=AX/4.0
228:        TSQ=T*T
229:        BJJZERO=-5.014415E-4
230:        BJJZERO=TSQ*BJJZERO+7.6771853E-3
231:        BJJZERO=TSQ*BJJZERO-7.09253492E-2
232:        BJJZERO=TSQ*BJJZERO+4.443584263E-1
233:        BJJZERO=TSQ*BJJZERO-1.7777560599
234:        BJJZERO=TSQ*BJJZERO+3.9999973021
235:        BJJZERO=TSQ*BJJZERO-3.9999998721
236:        BJJZERO=TSQ*BJJZERO+1.000000000
237:        RETURN
238:30      T=AX-7.853981634E-1
239:        S=SIN(T)
240:        C=COS(T)
241:        T=4.0/AX
242:        TSQ=T*T
243:        P=-3.7043E-6
244:        P=TSQ*P+1.73565E-5
245:        P=TSQ*P-4.87613E-5
246:        P=TSQ*P+1.734300E-4
247:        P=TSQ*P-1.7530620E-3
248:        P=TSQ*P+3.989422793E-1
249:        Q=-3.2312E-6
250:        Q=TSQ*Q+1.42078E-5
251:        Q=TSQ*Q-3.42468E-5
252:        Q=TSQ*Q+8.69791E-5
253:        Q=TSQ*Q-4.564324E-4
254:        Q=TSQ*Q+1.24669441E-2
255:        BJJZERO=P*C+T*Q*S
256:        T=SQRT(T)
257:        BJJZERO=T*BJJZERO
258:        RETURN
259:        END
260:        SUBROUTINE J1X(X,BJONE)
261:        IF (X) 5,10,15
262:5         AX=-X
263:        SIGN=-1.0
264:        GO TO 20
265:10       BJONE=0.0
266:        RETURN
267:15       AX=X
268:        SIGN=1.0
269:20       IF (AX-4.0) 25,25,30
270:25       T=AX/4.0
271:        TSQ=T*T
272:        BJONE=-1.289769E-4
273:        BJONE=TSQ*BJONE+2.2069155E-3
274:        BJONE=TSQ*BJONE-2.36616773E-2
275:        BJONE=TSQ*BJONE+1.777582922E-1
276:        BJONE=TSQ*BJONE-3.888839649E-1
277:        BJONE=TSQ*BJONE+2.6666660544
278:        BJONE=TSQ*BJONE-3.999999971
279:        BJONE=SIGN*T*(TSQ*BJONE+1.9999999998)

```

```
280:      RETURN
281:30    T=AX-7.853981634E-1
282:      S=SIN(T)
283:      C=COS(T)
284:      T=4.0/AX
285:      TSQ=T*T
286:      P=4.2414E-6
287:      P=TSQ*P-2.00920E-5
288:      P=TSQ*P+5.80759E-5
289:      P=TSQ*P-2.232030E-4
290:      P=TSQ*P+2.9218256E-3
291:      P=TSQ*P+3.989422819E-1
292:      Q=-3.6594E-6
293:      Q=TSQ*Q+1.62200E-5
294:      Q=TSQ*Q-3.98708E-5
295:      Q=TSQ*Q+1.064741E-4
296:      Q=TSQ*Q-6.390400E-4
297:      Q=TSQ*Q+3.74008364E-2
298:      BJONE=P*S+T*Q*C
299:      T=SQRT(T)
300:      BJONE=SIGN*T*BJONE
301:      RETURN
302:      END
:302
```

.ORRECTIONS APPLIED.

Appendix B. - Fortran program for determining the location (x, y, z coordinates) of the trapped miner.

```
000 DIM A(4,4),A1(4,4),B(4,4)S(4,4)C(4,4)Z(4)
005 B = 0
010 C = 0
015 F = 0
030 FOR I = 1 TO 4
040 PRINT "INPUT THE COORDINATES OF RECEIVER #";I
050 FOR J = 1 TO 3
060 PRINT "INPUT ";X$;" COORDINATE -> ";
070 INPUT A(I,J)
080 C(I,1) = C(I,1) + A(I,J) ^ 2 / 2
090 NEXT J
100 Z(I) = A(I,3)
110 F = F + Z(I) ^ 2
120 NEXT I
130 FOR I = 1 TO 4
140 PRINT "INPUT THE PHASE MEASUREMENT OF RECEIVER #";I
150 INPUT A(I,4)
160 A(I,3) = .5 * A(I,4) ^ 2
170 NEXT I
180 IF F = 0 THEN 310
190 PRINT "ESTIMATE THE DEPTH OF THE TRANSMITTER";
200 INPUT Z0
210 FOR I = 1 TO 4
220 B(I,1) = C(I,1) - Z(I) * Z0
230 NEXT I
240 A1 = INV(A)
250 S = A1 MPY B
260 X = S(1,1)
270 Y = S(2,1)
280 K = SQR (S(3,1))
290 D = S(4,1) / K
300 IF F = 0 THEN 1000
310 E = Z0 - SQR (D ^ 2 - X ^ 2 - Y ^ 2)
320 IF ABS (E / Z0) < .001 THEN 1000
330 Z0 = Z0 + E / 5
340 GOTO 310
1000 PRINT
1010 PRINT "X= ";X
1020 PRINT "Y= ";Y
1030 PRINT "Z= ";Z0
1040 PRINT "K= ";K
1050 PRINT "D= ";D
1060 PRINT "DO YOU WANT TO INPUT NEW PHASE MEASUREMENTS?";
1070 INPUT A$
1080 IF A$ = "Y" OR A$ = "YES" THEN 240
9999 END
```